Martin R. Prince, MD, PhD

Gadolinium-enhanced MR Aortography[1]

PURPOSE: **To evaluate the potential for preferential arterial enhancement at magnetic resonance (MR) aortography with an intravenous infusion of paramagnetic contrast material.**

MATERIALS AND METHODS: **Gadolinium chelates were administered intravenously (0.2 mmol/kg) during three-dimensional MR imaging (1.5 T) in 125 patients (77 male and 48 female patients, aged 4–86 years [mean, 66 years]) with suspected aorta or aortic branch vessel disease.**

RESULTS: **Infusion for the duration of the MR acquisition resulted in significant preferential arterial enhancement without the confounding effects of excessive venous or background-tissue enhancement ($P < 10^{-5}$). Angiographic or surgical correlation in 48 patients revealed an 88% sensitivity and a 97% specificity for detection of stenoses or occlusions and a 100% sensitivity and a 100% specificity for detection of aortic or iliac artery aneurysms.**

CONCLUSION: **Preferential arterial enhancement is possible at MR aortography with an intravenous infusion of paramagnetic contrast material.**

Index terms: Aorta, MR, 981.12943 • Magnetic resonance (MR), contrast enhancement, 981.12943, 9*.12943[2] • Magnetic resonance (MR), vascular studies, 981.12943, 9*.12943[2]

Radiology 1994; 191:155–164

[1] From the Department of Radiology, Massachusetts General Hospital, Harvard Medical School, Boston, Mass, and the Department of Radiology, University of Michigan, University Hospitals B1D530, Ann Arbor, MI 48109-0030. Received August 31, 1993; revision requested October 12; revision received November 4; accepted December 10. Supported in part by the RSNA Research and Education Fund as an RSNA Research Resident and by grant no. HL46384 from the National Institutes of Health. **Address reprint requests to** the author.

[2] 9* indicates generalized vein and artery involvement.

MAGNETIC resonance (MR) angiography is increasingly performed as a noninvasive method of evaluating patients with suspected vascular disease (1–3). MR angiography is particularly well suited to the evaluation of low-resistance vessels such as the carotid and intracerebral arteries. In healthy subjects, vessels of normal caliber have strong, continuous laminar flow, which is readily detected with standard time-of-flight techniques. But in patients with vascular disease that disturbs the normal laminar flow, time-of-flight images are degraded. There is loss of signal when inflow is reduced in ectatic vessels or in patients with low cardiac output. Tortuous vessels may have segments that are not oriented perpendicular to the plane of imaging, resulting in loss of signal from in-plane saturation. Loss of signal also results from turbulent dephasing in stenoses and aneurysms.

These problems are exacerbated in the abdomen and pelvis, where it is necessary to use a larger body coil, which results in a reduced signal-to-noise ratio. Peripheral arteries also have higher resistance with pulsatile, sometimes retrograde flow; this results in decreased blood signal and pulsatility artifacts. In addition, the considerable length of many peripheral vessels necessitates long imaging times with time-of-flight techniques because imaging must be performed in a plane perpendicular to the direction of flow.

This article describes a method of MR aortography that does not depend on blood inflow or blood motion and thereby circumvents many of the problems of conventional time-of-flight MR angiography. By administering a paramagnetic contrast agent intravenously, the T1 of blood is made short compared with that of fat (T1 = 270 msec), muscle (T1 = 600 msec), and other background tissues. It is then possible to image the arteries directly with excellent contrast and high resolution in a three-dimensional Fourier-transform acquisition optimized for the shortened T1 of the blood. The use of gadolinium chelates for enhancing MR angiography has been described in the intracranial circulation (4–9), aorta (10–13), and portal vein (14) and in popliteal-tibial vessels (15). The previously reported problems of background tissue and venous enhancement were avoided in this study by imaging during infusion of contrast material. In addition to demonstrating the technique, this article evaluates the effects of infusion time, dose, and differences between three currently available gadolinium compounds.

MATERIALS AND METHODS

Theory

Gadolinium chelates are paramagnetic agents that shorten the spin-lattice relaxation time, T1, of blood according to the equation

$$\frac{1}{T1} = \frac{1}{1{,}200} + R \times [Gd], \qquad (1)$$

where 1/1,200 is the T1 of blood without gadolinium, R is the relaxivity, and [Gd] is the blood concentration of a gadolinium chelate.

During dynamic imaging at times shorter than the recirculation time, the blood concentration of a gadolinium chelate is determined by the intravenous infusion rate and the cardiac output as

$$[Gd]_{arterial} = \frac{\text{Gd infusion rate}}{\text{cardiac output}}. \qquad (2)$$

The three gadolinium chelates currently available for clinical use were investigated in this study: gadopentetate dimeglumine (Magnevist; Berlex Laboratories, Wayne, NJ), gadoteridol (Prohance; Squibb Diag-

Abbreviations: MIP = maximum intensity projection, SI = signal intensity, TE = echo time, TR = repetition time.

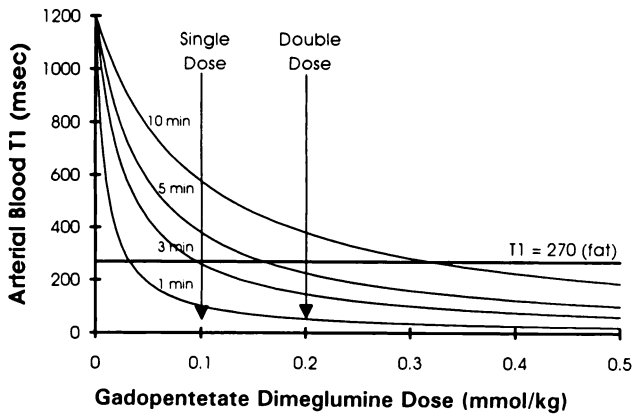

1.

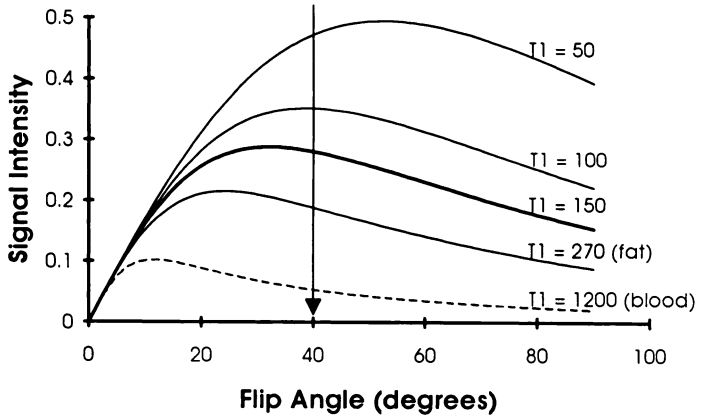

2.

Figures 1, 2. **(1)** Graph depicts predicted blood T1 versus total dose of gadopentetate dimeglumine for infusion times of 1, 3, 5, and 10 minutes, assuming a negligible venous accumulation and a relaxivity of 4.5 $msec^{-1} \cdot mmol^{-1}$. Note that for infusion times of 3–5 minutes, a double dose is required to make the T1 of arterial blood less than the T1 of fat. **(2)** Graph depicts predicted relative SI versus flip angle for a spoiled gradient-echo sequence with TR of 25 msec and TE much less than T2*, for tissues of various T1. A flip angle of about 40° is optimal for maintaining a high SI and for maximizing the SI difference between arterial blood (predicted T1, 100–150 msec) and fat (T1, 270 msec).

nostics, Princeton, NJ), and gadodiamide injection (Omniscan; Sanofi Winthrop Pharmaceuticals, New York, NY); the relaxivities are about 4.5 $msec^{-1} \cdot mmol^{-1}$. Assuming a constant infusion rate, combining Equations (1) and (2) predicts the arterial blood T1 as a function of infusion time and total gadolinium administered (Fig 1). For contrast material infusion times that are longer than the recirculation time, the arterial blood T1 will be even shorter, since a large fraction of the injected gadolinium chelate will recirculate. From Figure 1, it is apparent that the shortest T1 occurs with the shortest infusion time and the largest dose of gadolinium chelate. For the typical imaging times of 3–5 minutes, Figure 1 shows that the dose must be at least 0.2 mmol/kg to achieve a blood T1 substantially shorter than that of the brightest background tissue, fat (T1 = 270 msec).

With a gadolinium chelate dose of 0.2 mmol/kg and a 3–5-minute infusion during imaging time, the arterial blood T1 is predicted to be 150–200 msec. It will actually be shorter since the recirculation time is less than 3–5 minutes. The relative signal intensity (SI) in a three-dimensional Fourier-transform spoiled gradient-echo acquisition as a function of blood T1, repetition time (TR), T2* flip angle, α, and proton density ($N[H]$) can be calculated with Equation (3) (16).

$$SI = N(H)\frac{1 - \exp\left(-\frac{TR}{T1}\right)}{1 - \cos(\alpha) \cdot \exp\left(-\frac{TR}{T1}\right)} \cdot \sin(\alpha) \cdot \exp\left(-\frac{TE}{T2^*}\right). \quad (3)$$

For a TR of 25 msec and assuming the echo time (TE) is small compared with T2*, the relative SI is plotted in Figure 2 for T1 of 100, 150, 200, and 270 (fat) msec. This shows that a flip angle of about 40° is optimal for maximizing blood-to-background tissue (fat) contrast.

Patients

Gadolinium-enhanced MR arteriography was performed in 125 patients referred for routine MR angiography of the aorta or branch vessels. The patients included 77 male and 48 female patients, aged 4–86 years (mean, 66 years). The main criteria for enrollment in the study included aortic aneurysm (n = 33), hypertension and/or renal failure (n = 67), and claudication (n = 19). The patients were divided into four groups, reflecting the chronological development of the technique.

Group 1 comprised 12 patients who underwent dynamic imaging after bolus injection of 0.2 mmol/kg gadopentetate dimeglumine during the first 1–2 minutes of a 5 minute 8 second acquisition. Group 2 comprised 25 patients who underwent dynamic imaging during continuous infusion of 0.2 mmol/kg gadopentetate dimeglumine over a 5 minute 8 second acquisition. A subset of this data (16 patients) has been reported previously (10). Group 3 comprised 19 patients who underwent dynamic imaging during continuous infusion of 0.2 mmol/kg gadopentetate dimeglumine over a 3 minute 18 second acquisition. Group 4 comprised 69 patients who underwent dynamic imaging during continuous infusion of a fixed dose of 40 mL gadopentetate dimeglumine (0.5 mol/L), gadoteridol (0.5 mol/L), or gadodiamide injection (0.5 mol/L) over a 3 minute 18 second acquisition. Subgroup 4a included 15 of these patients who underwent imaging before, during, and after infusion of gadopentetate dimeglumine to assess the dynamics of vascular enhancement.

Imaging Parameters

All imaging was performed on a 1.5-T superconducting magnet (GE Medical Systems, Milwaukee, Wis), with use of the body coil and 4.7 software. First, a sagittal or coronal T1-weighted localizer image was obtained that was centered on the xiphoid. Then a three-dimensional Fourier-transform spoiled gradient-echo volume was acquired that was centered on the arteries of interest. For groups 1 and 2, the imaging parameters were 9–12-cm-thick sections with 60 partitions (1.5–2.0-mm partition thickness) oriented with the arteries in plane (ie, coronal for aortoiliac disease and sagittal for the thoracic aorta), TR of 25 msec, TE of 6.9 msec (where fat and water are out of phase), flip angle of 40°, first-order flow compensation, 32–40-cm field of view, and 256 × 192 matrix. No saturation pulses were employed. The imaging time was 5 minutes 8 seconds. In groups 3 and 4, the number of partitions was 28 with 2-mm partition thickness, the matrix was 256 × 256 with a 36-cm field of view, the TE remained the same (6.9 msec), and the TR was 24 msec, resulting in a higher-resolution image and a shorter imaging time of 3 minutes 18 seconds. With this three-dimensional pulse sequence, k space was acquired in the standard linear fashion, in which the partitions are encoded sequentially and, for each partition, the lines of k space are acquired from bottom to top (negative to positive).

In 38 of 125 patients, conventional unenhanced time-of-flight images were available for comparison. For renal MR angiography, a multiple overlapping thin slab acquisition was performed as a gradient-echo steady-state pulse sequence in the axial plane, centered on the renal arteries. The following parameters were used: TR of 29 msec, TE of 6.9 msec, 20° flip angle, first-order flow compensation, 1.5-mm partition thickness, 16 partitions per slab with 50% overlap of the slabs, 32-cm field of view, 256 × 128 matrix, and two signals averaged. Inferior presaturation pulses were used to suppress venous inflow. The total imaging time was 11 minutes 59 seconds to cover 7.8 cm of aorta in the superior-to-inferior dimension.

For iliac MR angiography, a two-dimensional time-of-flight acquisition was performed with a gradient-echo steady-state

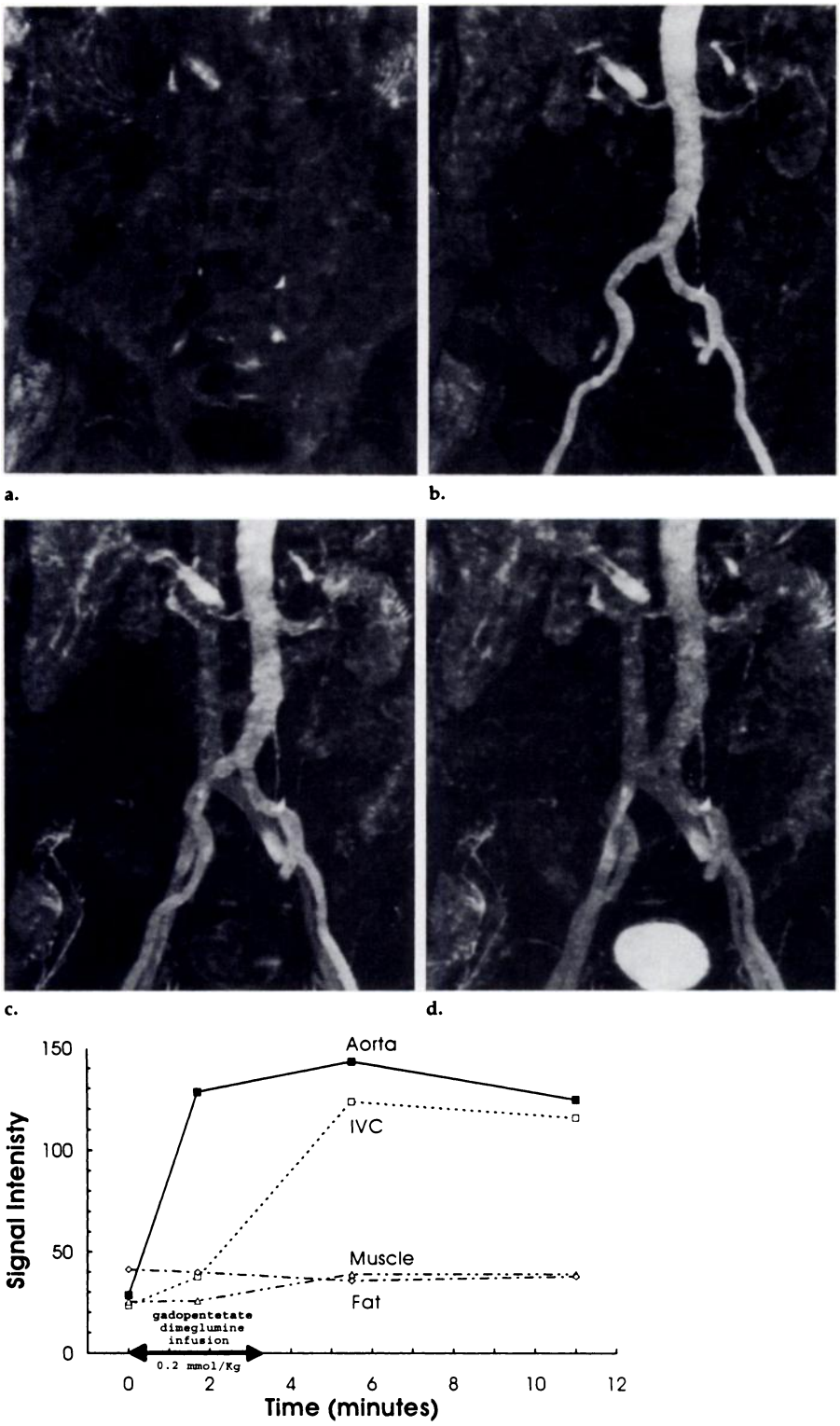

Figure 3. Typical MIP images from three-dimensional data sets obtained **(a)** before, **(b)** during, **(c)** immediately after, and **(d)** 5 minutes after infusion of gadopentetate dimeglumine (0.2 mmol/kg) for the duration of a 3 minute 18 second three-dimensional Fourier-transform coronal acquisition. **(e)** Graph depicts these changes in vascular and background tissue SI. Note that the precontrast image shows no vascular enhancement, while during infusion of gadopentetate dimeglumine there is dramatic arterial enhancement but minimal enhancement of the inferior vena cava (*IVC*) and after infusion there is both arterial and venous enhancement. Image in **d** shows contrast material beginning to accumulate in the bladder.

pulse sequence in the axial plane with the following parameters: TR of 29 msec, TE of 6.9 msec, flip angle 45°, first-order flow compensation, 32-cm field of view, 256 × 192 matrix, 2.9-mm section thickness, and one or two signals averaged. Inferior presaturation pulses were used to suppress venous inflow. The total imaging time was 7 minutes 31 seconds or 15 minutes 2 seconds to cover 23 cm of aorta and iliac artery, respectively, in the superior-to-inferior dimension.

Gadolinium Infusion

Venous access was obtained via a 22-gauge peripheral intravenous catheter, usually in the forearm or antecubital fossa. A dynamic acquisition was then performed during hand infusion of the gadolinium chelate. In group 1, a 0.2 mmol/kg (17) bolus injection of gadopentetate dimeglumine was begun within 5 seconds of starting the acquisition and was completed within the first 1–2 minutes of the 5-minute imaging time. In groups 2, 3, and 4, the infusion was carefully timed to begin within 5–10 seconds after commencing the acquisition and to end 10–20 seconds before the end of the acquisition. A 5–20-mL injection of normal saline solution was given to ensure infusion of the entire dose of chelate. For comparison, subgroup 4a underwent imaging with identical acquisitions before, during, and after infusion of gadopentetate dimeglumine without altering the imaging parameters.

Image Reconstruction

Maximum intensity projection (MIP) acquisitions in cardinal planes and multiplanar reformations were performed at the independent workstation (Signa; GE Medical Systems). Subvolume MIP acquisitions in arbitrary planes were performed at a different computer workstation (SPARC 10-41-2GX; Sun Microsystems, Sunnyvale, Calif) with AVS software (Advanced Visual Systems, Waltham, Mass).

SI Measurements

SI was measured in all patients in the aorta, inferior vena cava, and background tissues (fat and skeletal muscle) for at least three regions of interest per measurement. Since the imaged volume was entirely within the patient in virtually every case, it was not possible to measure noise from a region of interest outside the patient. Instead, an alternative measurement was made on a region within the image volume that was chemically and structurally homogeneous to the MR resolution of aortic blood. All SI measurements were divided by the standard deviation of the signal within the aorta to give an SI ratio that is analagous to the signal-to-noise ratio. The SI ratio is actually an underestimate of the true signal-to-noise ratio because the standard deviation of the aortic signal may be increased not only by true noise but also by flow phenomena and phase artifacts. In subgroup 4, additional SI measurements were obtained in the iliac, renal, portal, and hepatic veins and in the kidney, liver, and spleen. Identical regions of interest were used on the images ob-

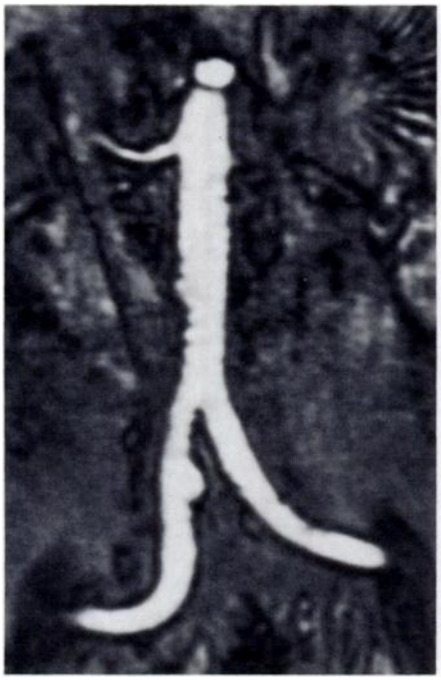

Figure 4. Raw-data coronal image shows the origin of the right renal artery, an aneurysm on the right common iliac artery, and mural irregularity of the distal abdominal aorta.

tained before, during, and after administration of contrast material.

Correlations

In 48 patients, conventional arteriography or surgery was performed after gadolinium-enhanced MR angiography. In these patients, it was possible to evaluate the prospective accuracy of MR angiography by comparing the descriptions of vessels and vessel disease on the MR angiography report with the descriptions on the conventional angiography reports and operative notes. The interpretation of the images in each case was performed by an angiography fellow together with a staff angiographer, with consultation from other staff in difficult cases, to generate a single final report representing a consensus opinion. Findings at conventional angiography or surgery were considered the standards of reference. In the reports, arteries were graded as aneurysmal, occluded, or stenotic. Stenoses were graded as mild, moderate, or severe. Mild was considered negative for statistical purposes. Vessels that were not described in both the MR angiography report and either the conventional angiography report or operative note were excluded from this analysis.

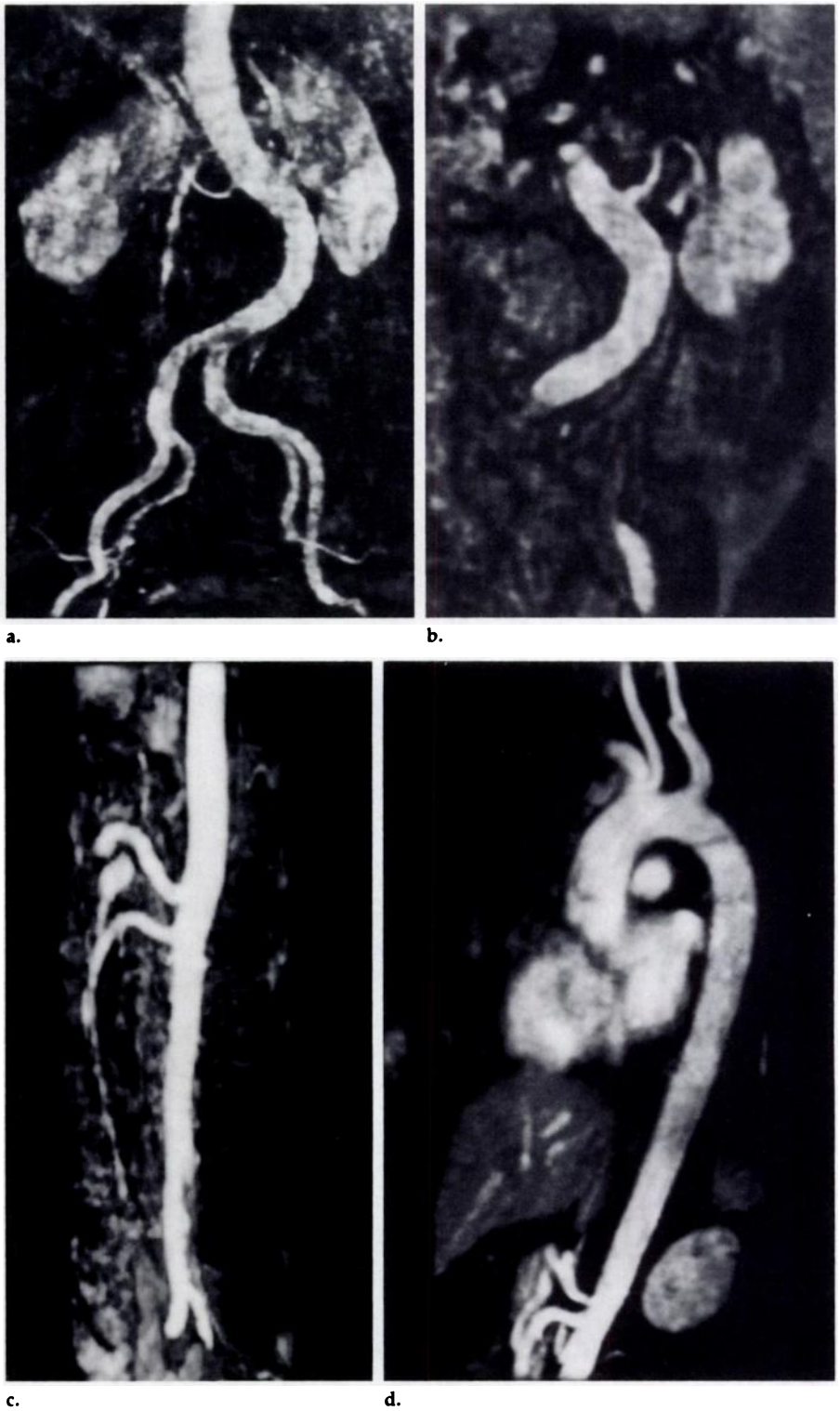

Figure 5. **(a)** A coronal MIP collapsed image of an entire data set and **(b)** a subvolume MIP optimized image of the left renal artery were obtained in one patient. **(c)** A subvolume MIP optimized image of the celiac trunk and superior mesenteric artery and **(d)** a subvolume MIP optimized image of the aortic arch were obtained in two different patients.

Statistical Analysis

Differences in the aortic SI and contrast ratios for each of the techniques and contrast agents were evaluated with the Student *t* test. The significance of differences in the mean SI of the portal, hepatic, renal, or iliac veins compared with that of the inferior vena cava and differences in aorta SI ratio during infusion of contrast material compared with that on precontrast images were evaluated with the Student *t* test for paired data. For the angiographic and surgical correlations, sensitivity for detecting aneurysms and for detecting stenoses or occlusions was calculated as the number of true-positive findings at MR angiography divided by the number of positive findings at conventional angiography or surgery. Specificity was calculated as the number of true-negative findings at MR angiography divided by the number of negative findings at conventional angiography or surgery.

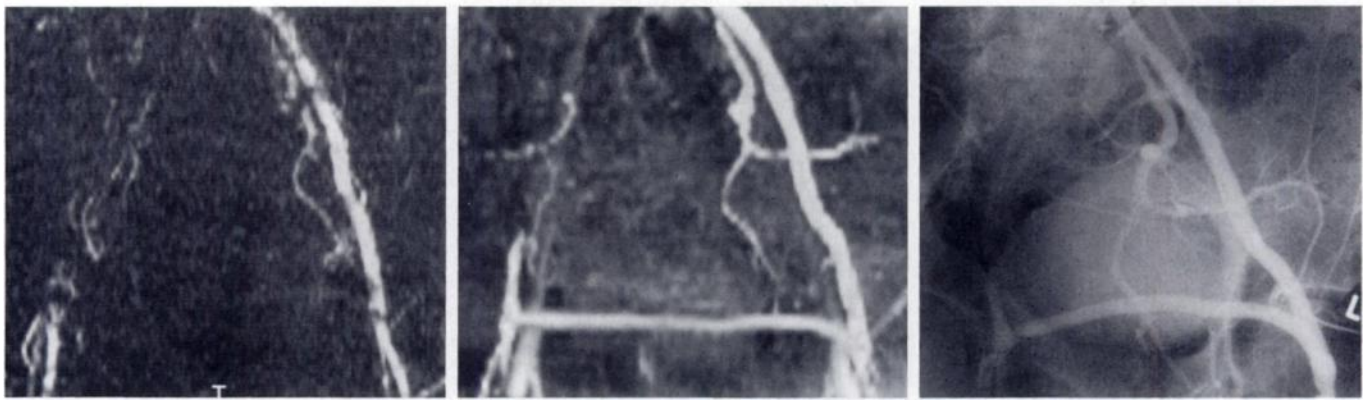

Figure 6. **(a)** Two-dimensional time-of-flight and **(b)** dynamic gadolinium-enhanced MR angiograms and **(c)** conventional arteriogram were obtained in a patient with an occluded right iliac system bypassed with a femoral artery–to–femoral artery graft. Note that the graft is not seen in **a** because of in-plane saturation but that it is well seen in both **b** and **c**.

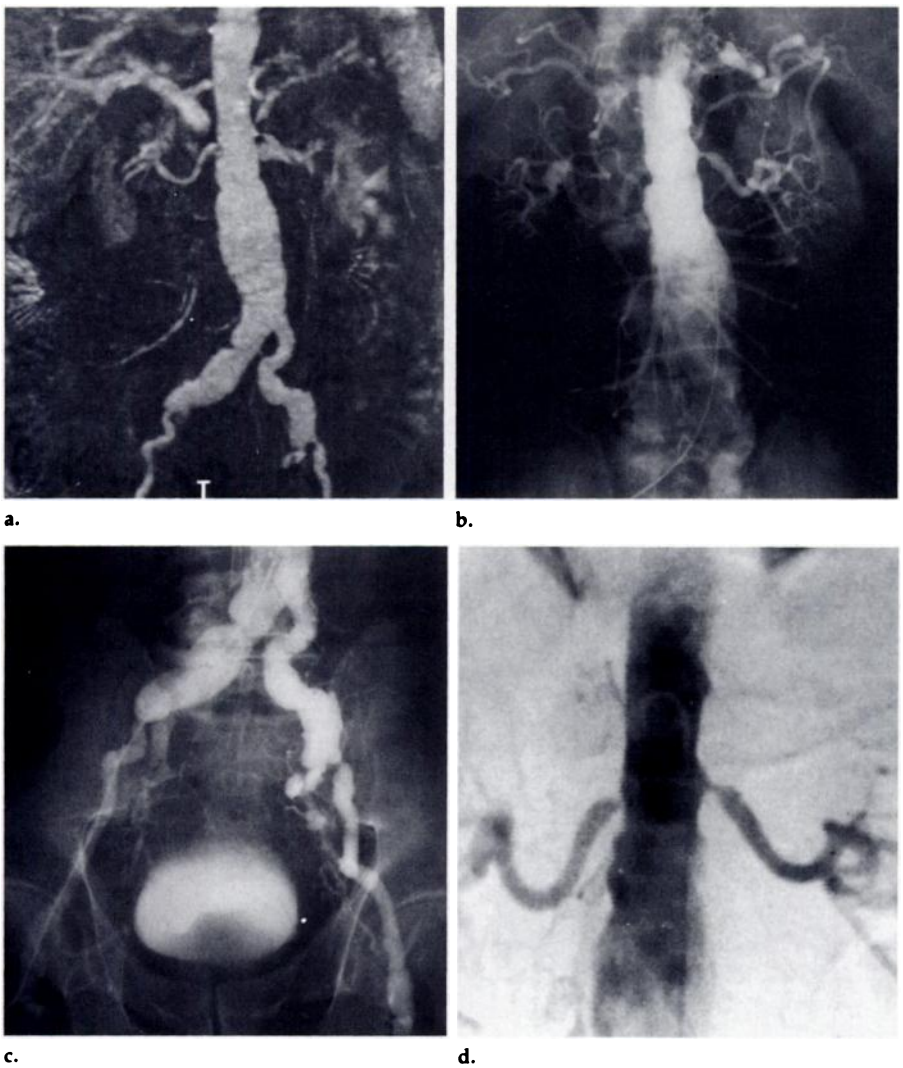

Figure 7. **(a)** Gadolinium-enhanced MIP MR angiogram depicts an abdominal aortic aneurysm extending into the iliac arteries and bilateral severe renal artery stenoses. **(b–d)** Conventional angiograms help confirm MR findings. The left renal artery is partially obscured by renal vein enhancement in **a**, but it can be seen in greater detail on the raw-data and reformatted images (not shown).

RESULTS

Figure 3 illustrates the typical images obtained before, during, and after intravenous infusion of a gadolinium chelate (0.2 mmol/kg). Images obtained before the infusion show saturation of the blood vessels throughout most of the volume, with short segments of bright vessels at the edges of the image volume. Images obtained during the infusion show enhancement of the arteries while the inferior vena cava remained indistinguishable from the background tissues. Images obtained after the end of the infusion demonstrate comparable enhancement of arteries and veins. These changes in SI are shown graphically in Figure 3e.

These three-dimensional data sets with near isotropic voxels could be viewed in many ways in addition to the total-volume MIP images shown in Figure 3. The raw data could be reviewed one section at a time (Fig 4). Digital subtraction of the precontrast data from the data obtained during infusion was generally not effective at improving image quality, because of misregistration. The data set could be sectioned in any arbitrary plane to view, for example, the origins of the superior mesenteric artery and celiac axis or a renal artery in a single plane. Subvolume MIP imaging allowed visualization of arteries that did not conform to a single 1-voxel-thick plane (Fig 5).

The gadolinium-enhanced images showed no evidence of the in-plane saturation that degraded time-of-flight images (Fig 6). Arteries with blood flowing in opposite directions were visible on the same image (Fig 5a). The aorta and iliac artery aneurysms were particularly well seen, owing to their large size. The enhancement within aneurysms was comparable with that of arteries of normal caliber (Figs 4, 7, 8), even though their SI on the standard time-of-flight images was severely degraded.

Although all major arteries en-

hanced comparably, there were large differences in the degree of enhancement of different veins on the dynamic images. The portal vein was the brightest, followed by hepatic and renal veins. The iliac veins and infrarenal inferior vena cava were indistinguishable from background tissues. These differences are quantitated in Table 1. Gadolinium significantly increased the aortic SI ratio from 2.3 to 10.0 ($P < .00001$) compared with an increase from 1.8 to 3.1 in the inferior vena cava. In postcontrast images, however, the aorta and inferior vena cava had similar SI ratios of 12 and 10, respectively. Muscle enhanced minimally during infusion (×1.1) but had enhanced substantially by the time a postcontrast acquisition was performed (×1.8). Fat, interestingly, had slightly decreased SI on the images obtained during and after infusion compared with the SI on precontrast images, presumably representing improved canceling of fat signal with the opposed-phase technique. Vascular tissues enhanced noticeably during and after infusion, including kidney (×2.7), spleen (×2.3), and liver (×1.6) (Table 1).

The image time and infusion timing had a significant effect on the image quality and on the ratio of arterial-to-venous enhancement. Injection of contrast material as a bolus during the first 1–2 minutes of a 5-minute acquisition resulted in only a minimal difference between aortic and inferior vena caval enhancement, with an aorta-to–inferior vena cava SI ratio of 1.2 (Table 2). By infusing the gadolinium chelate over the acquisition time, beginning after the acquisition commenced and ending 20 seconds before the acquisition ended, the aorta-to–inferior vena cava SI ratio increased to 2.5 within the same 5-minute acquisition. By reducing the imaging time to 3 minutes 18 seconds, a further improvement was observed in aorta-to–inferior vena cava SI ratio to 2.8. Interestingly, use of the shorter imaging times with a faster infusion rate did not diminish the aortic SI ratio or contrast ratios.

Qualitatively, higher doses of gadolinium chelates resulted in improved arterial enhancement. The effect of dose on aortic SI ratio is illustrated quantitatively in Figure 9 for the group 4 patients receiving gadopentetate dimeglumine over a 3 minute 18 second acquisition. Although all three gadolinium chelates have comparable relaxivities ($\sim 4.5\ msec^{-1} \cdot mmol^{-1}$) and similar pharmacokinetics, gadodiamide injection produced marginally better aortic enhancement (Table 3). The gadodiamide injection–enhanced aortic SI ratio of 11.9 ± 2.6 (mean ± standard deviation) was significantly higher than for gadopentetate dimeglumine (10.8 ± 2.2) and gadoteridol (10.7 ± 2.4) ($P = .05$). There was no significant correlation detected between aortic SI ratio and serum creatinine level or age. Female patients had a significantly higher aortic SI ratio than male patients (11.9 ± 2.3 vs 10.7 ± 2.4) ($P = .03$). This could be accounted for by the difference in mean weight between the male patients (mean weight, 176 lb [79.2 kg]) and female patients (mean weight, 132 lb [59.4 kg]), which resulted in female patients receiving a higher dose per weight, on average.

Table 2 also shows how the time-of-flight images compare quantitatively with the gadolinium-enhanced MR angiograms. The multiple overlapping thin slab acquisition and two-dimensional Fourier-transform techniques required five to 20 times longer to image the same length of aorta, even with use of larger voxel volumes. SI and contrast ratios for the gadolinium-enhanced images were comparable with those for the time-of-flight images.

Angiographic and/or surgical correlation was available in 48 of the 125 patients (Table 4). In the vascular seg-

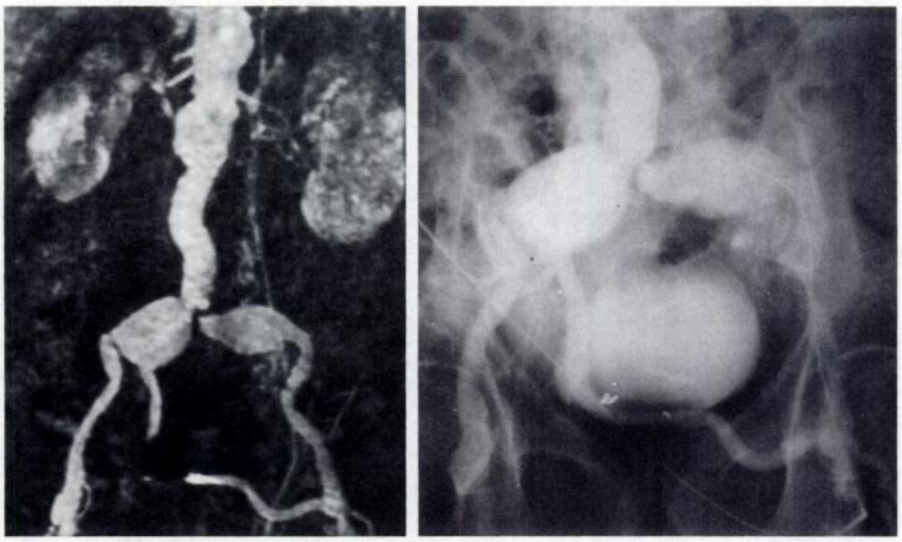

a. b.

Figure 8. **(a)** Gadolinium-enhanced MR angiogram shows bilateral iliac artery aneurysms, a stenosis at the origin of the left common iliac artery, and an aortic tube graft with an aorto-femoral limb. **(b)** Conventional angiogram helps confirm these findings. Note that surgical clip artifacts are not avoided in **a.**

Table 1
Average Tissue SI (Normalized to Aortic Noise)

Tissue	SI before Infusion	SI during Infusion	SI after Infusion	Ratio during Infusion: Before Infusion	Ratio during Infusion: Aorta*
Blood vessels					
Aorta	2.3 ± 0.7	10.0 ± 2.1	12.0 ± 3.3	4.2	1.0
Inferior vena cava	1.8 ± 0.5	3.1 ± 1.5	10.0 ± 2.8	1.7	0.3
Iliac vein	1.7 ± 0.3	2.8 ± 1.4	9.4 ± 3.0	1.7	0.3
Renal vein	1.8 ± 0.7	5.6 ± 1.7	10.0 ± 3.1	3.0	0.6
Portal vein	3.4 ± 2.6	8.4 ± 3.3	12.0 ± 3.3	2.6	0.8
Hepatic vein	3.1 ± 1.1	6.8 ± 5.4	14.0 ± 4.7	2.2	0.7
Background					
Kidney	2.3 ± 0.6	6.3 ± 1.6	7.6 ± 2.3	2.7	0.6
Liver	2.9 ± 1.0	4.6 ± 1.5	6.5 ± 1.9	1.6	0.5
Spleen	2.4 ± 0.9	5.5 ± 1.5	8.0 ± 2.9	2.3	0.6
Fat	4.0 ± 0.8	3.7 ± 0.6	3.1 ± 0.4	0.9	0.4
Muscle	1.8 ± 0.6	1.9 ± 0.6	3.0 ± 0.8	1.1	0.2

Note.—Values determined at MR angiography in 15 subjects for 3 minute 18 second acquisitions performed before, during, and after infusion of 40 mL gadopentetate dimeglumine. Numbers are mean ± standard deviation.

* SI of tissue during infusion divided by SI of aorta during infusion.

Table 2
Effect of Injection Method and Rate on Aortic SI and Contrast Ratio

Group	Injection Method	Imaging Time	Imaging Time per Centimeter (sec/cm)	Voxel Volume (mm^3)	SI Ratio		Contrast Ratio†	
					Aorta*	Aorta/Inferior Vena Cava	Aorta/Fat†	Aorta/Muscle†
Two-dimensional time-of-flight (n = 11)	None	7 min 31 sec	20.0	6.0	6.8 ± 2.8	5.6 ± 2.4	4.8 ± 2.2	5.6 ± 2.3
Multiple overlapping thin slab acquisition (n = 27)	None	11 min 59 sec	92.0	4.7	10.0 ± 3.0	2.7 ± 1.0	5.3 ± 2.2	7.3 ± 2.2
1 (n = 12)	Bolus	5 min 8 sec	9.0	3.1	12.0 ± 2.4	1.2 ± 0.2	7.5 ± 1.6	9.1 ± 1.9
2 (n = 25)	Infusion	5 min 8 sec	9.0	3.1	9.7 ± 1.2	2.0 ± 0.5	5.4 ± 1.1	7.6 ± 1.1
3 (n = 19)	Infusion	3 min 18 sec	5.5	3.1	1.0 ± 2.0	2.4 ± 0.8	6.8 ± 1.9	8.1 ± 1.7

Note.—Gadolinium chelate is gadopentetate dimeglumine.
* Aorta SI ratio = (aorta SI)/(standard deviation of aorta/SI).
† Aorta/tissue contrast ratio = (aorta SI − tissue SI)/(standard deviation of aortic SI).

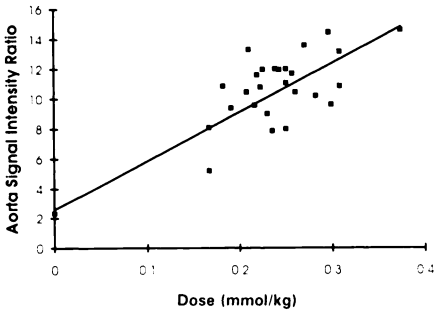

Figure 9. Graph depicts SI ratio of aorta as a function of dose of gadolinium chelate. Aorta SI increased with increasing dose (r = .75).

ments for which definitive correlation was available, MR arteriography clearly depicted all 39 aortic and iliac artery aneurysms. Aortic and branch vessel stenoses and occlusions were depicted with an overall 88% sensitivity and 97% specificity. This technique was best for evaluating larger arteries, with 100% sensitivity and 100% specificity in evaluating the aorta and 94% sensitivity and 98% specificity in evaluating the iliac arteries. Accuracy dropped off in smaller arteries, with 85% sensitivity and 93% specificity in evaluating the renal arteries. There were too few lesions of the great vessels, celiac artery, or superior and inferior mesenteric arteries for those data to be meaningful.

Normal renal arteries were often seen in sufficient detail that the referring physicians chose not to pursue angiographic confirmation. In two patients with hypertension and elevated creatinine level, MR angiography depicted severe stenoses and renal revascularization was performed without performing conventional angiography. In both cases, renal function and blood pressure control improved postoperatively. Four renal artery lesions were missed at MR angiography that were found at conventional angiography. These lesions included two moderate stenoses that were not believed to be clinically significant. One of the severe stenoses was in a right renal artery of a patient with a severe stenosis detected at MR angiography in another right renal artery. The other stenosis was an isolated severe stenosis in one of two left renal arteries. Thus, MR angiography failed to depict marked renovascular disease in only one of 29 cases with angiographic or surgical correlation. Two false-positive findings included one lesion graded mild at angiography that was graded severe at MR angiography and a normal renal artery graft that artifactually appeared stenotic at MR angiography. Of 29 cases with angiographic or surgical correlation, five supernumerary renal arteries were correctly identified, five were missed, and one was described at MR angiography but was not found at conventional angiography.

There was a single false-negative finding in an iliac artery at MR angiography of a moderate stenosis in a common iliac artery described as patent at MR angiography. A single false-positive finding in an iliac artery was in a tortuous external iliac artery described as moderately stenotic at MR angiography and as patent at conventional angiography. One interesting pitfall occurred in a normal subclavian artery at conventional angiography that was incorrectly identified as stenotic at dynamic gadolinium-enhanced MR angiography (Fig 10). This artery was adjacent to the vein draining the site of contrast material infusion. Retrospective evaluation of the images identified a susceptibility artifact around the subclavian vein due to the extremely high gadolinium concentration, which was causing artifactual loss of signal in the adjacent subclavian artery.

The patients tolerated the imaging and gadolinium chelates well; there were no allergic reactions to the contrast material. No patient had a deterioration in renal function attributable to the contrast material. Extravasation of 30 mL gadopentetate dimeglumine (osmolality, 1,960 mosm/kg water) at the infusion site (antecubital fossa) occurred in one patient. This was initially painful, but all symptoms resolved within 1 hour with gentle massage and application of a warm compress. Extravasation of 40 mL gadoteridol (osmolality, 630 mosm/kg water) occurred in one patient. There was a lump at the extravasation site in the antecubital fossa, but the patient indicated that it was not painful; the lump resolved within 1 hour with gentle massage with no adverse sequelae.

DISCUSSION

Time-of-flight MR imaging techniques are increasingly used to evaluate vascular anatomy and disease. Their value can be limited, however, in diseased vessels in which the time-of-flight MR signal is degraded by slow, turbulent, or in-plane flow. These data in 125 patients demonstrate an MR angiography technique that does not depend on blood inflow. By imaging dynamically during the continuous infusion of paramagnetic contrast material, there is selective visualization of arteries without degradation from slow or in-plane flow or the swirling flow within aneurysms and without the confounding effects of excessive venous or background tissue enhancement.

Since dynamic gadolinium-enhanced MR angiography does not depend on the inflow of unsaturated spins, the saturation problems that complicate routine time-of-flight im-

Table 3
Comparison of SI with Three Gadolinium Chelates

Gadolinium Chelate	Mean Dose (mmol/kg)	SI Ratio*		Contrast Ratio†		
		Aorta*	Inferior Vena Cava	Aorta/Inferior Vena Cava‡	Aorta/Fat	Aorta/Muscle
Gadopentetate dimeglumine (n = 27)	2.5	10.8 ± 2.2	2.8	6.3	7.0	8.8
Gadoteridol (n = 20)	2.5	10.7 ± 2.4	2.5	5.9	6.3	8.5
Gadodiamide injection (n = 22)	2.4	11.9 ± 2.6‡	3.2	7.6	7.6	9.7

Note.—Infusions were 40 mL of contrast material over 3 minute 18 second imaging time.
* Aorta SI ratio = (aorta SI)/(standard deviation of aortic SI).
† Aorta/tissue contrast ratio = (aorta SI − fat SI)/(standard deviation of aortic SI).
‡ Significantly different from gadopentetate dimeglumine and gadoteridol (P = .05).

aging are eliminated. It is possible to image in any plane without concern for saturation. The imaging volume can be oriented for optimal coverage of the vessels of interest with a minimum of imaging time (coronal imaging for aortoiliac disease or axial imaging for the subclavian arteries). It is possible to use three-dimensional Fourier-transform imaging with its intrinsically high spatial resolution and high signal-to-noise ratio (18–22). Turbulent and/or slow flow such as occurs in abdominal aortic or iliac artery aneurysms (Figs 4, 7, 8) is not a problem. Preferential enhancement of the arteries simplifies analysis by minimizing the confusion caused by overlapping veins. The resulting images are remarkably similar to those obtained with conventional arteriography.

This technique is particularly useful for evaluating aortic and iliac artery aneurysms. Aneurysms have been difficult to image at MR angiography because the slow swirling flow within aneurysms degrades both time-of-flight and phase-contrast images. Large aneurysms can also be problematic for conventional, catheter-based aortography because of the large amount of iodinated contrast material required to fill the entire aneurysm and because vessel tortuosity may cause overlap on conventional arteriograms. These problems are eliminated with this dynamic gadolinium-enhanced MR angiographic technique. The three-dimensional algorithm allows reformatting the data sets into any plane for optimal unfolding of tortuous vessels. The aortic and iliac artery anatomy was defined with sufficient detail to allow proceeding to aorta and/or iliac artery aneurysm repair in eight cases, without performing conventional angiography. In these cases, all patients had elevated serum creatinine levels or other relative contraindications to conventional arteriography.

Table 4
Arterial Stenoses and Occlusions Found at MR Angiography, with Surgical Correlation

Vessel	Sensitivity	Specificity	No. of Moderate Stenoses	No. of Severe Stenoses	No. of Occlusions
Aorta and great vessels (n = 25)	1.00	0.94	4	2	2
Iliac artery (n = 64)	0.94	0.98	9	3	3
Celiac trunk (n = 18)	0.80	0.92	4	0	1
Proximal superior mesenteric artery (n = 18)	0.50	1.00	1	0	0
Proximal renal artery (n = 59)	0.85	0.93	9	11	7
All arteries (n = 186)	0.88	0.97	27	16	13

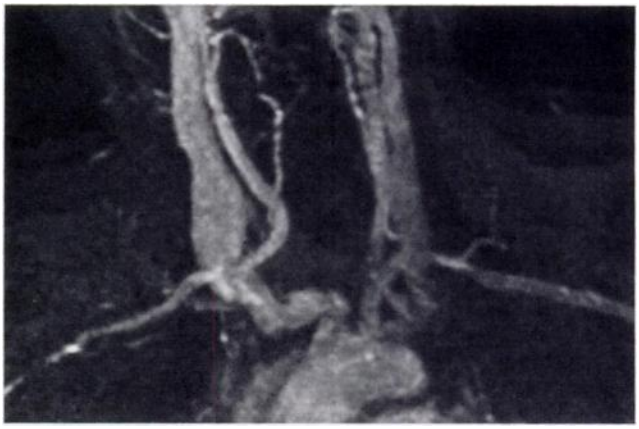

Figure 10. MIP image of coronal images centered on the aortic arch shows enhancement of the arch and carotid arteries with no visualization of the external jugular vein, but the internal jugular veins enhance comparably with the carotid arteries. Presumably this is because the blood-brain barrier prevents extraction of gadolinium chelate in the intracerebral circulation. Note also that the right subclavian artery is artifactually narrowed due to a susceptibility effect from the high concentration of gadolinium chelate in the adjacent vein, which drains the site of infusion.

Gadolinium-enhanced MR angiography is now routinely performed at Massachusetts General Hospital to screen for renal artery stenosis in patients with renal failure and/or hypertension that is difficult to control. The reported absence of renal toxicity (23,24) is confirmed by findings in this study, even in patients with elevated creatinine levels. The 85% sensitivity and 93% specificity for detecting renal artery stenoses compares favorably with those in previous reports of renal MR angiography (25,26). The confidence with which interpretations can be rendered is reflected in the

clinician's decisions in two cases to undertake surgical renovascular reconstruction without confirmation at conventional arteriography.

The tomographic nature of the data with image contrast derived from carefully timed intravenous infusions makes this technique similar to helical computed tomography (CT). Gadolinium-enhanced MR angiography has many advantages over helical CT, including (*a*) use of safer contrast media with no nephrotoxicity and fewer idiosyncratic reactions, (*b*) no risk from ionizing radiation, (*c*) no bone or calcified arterial plaque masquerades as contrast material, (*d*) imaging is possible in any plane for optimal in-plane coverage of the vessel of interest, and (*e*) higher resolution with isotropic voxels is possible. The main disadvantage of gadolinium-enhanced MR angiography is the longer imaging time, which allows respiratory motion to degrade the images. There are also important contraindications to MR imaging, including the presence of implanted electronic devices (such as pacemakers) or orbital shrapnel and claustrophobia. The presence of metallic artifacts from surgical clips and implants may be problematic in imaging with either technique.

The 3–5-minute duration of the infusion during imaging is too long to explain the absence of venous enhancement simply as a first-pass bolus effect. One hypothesis is that the intraarterial gadolinium chelate is extracted from the intravascular space as it passes through the systemic capillary bed. This net transfer of contrast material into the extracellular fluid compartment combined with continuous administration results in the venous level being less than the arterial level for the entire duration of the infusion. Visualization of the internal jugular and intracerebral veins can be explained as a result of the blood-brain barrier preventing extraction of the gadolinium chelate in the intracerebral circulation. Another contributing factor might be the transit time through the systemic capillary beds. This could explain why the iliac veins have lower signal than the renal, portal, and hepatic veins, all of which have much faster blood transit times. Another hypothesis is that the acquisition of the center of k space is matched to the period of maximum effect of the first-pass bolus.

Timing of the infusion of contrast material had a major effect on the degree of differential enhancement between the aorta and the inferior vena cava. Early injection (group 1) resulted in a minimal aorta-to–inferior vena cava contrast differential. A two- to fourfold aorta-to–inferior vena cava differential in SI ratio was achieved by infusing slowly, starting immediately after the beginning of imaging and finishing 20 seconds before the end of the acquisition, being especially careful not to slow down the infusion during the middle of the acquisition (groups 2–4). By avoiding early injection of too much contrast material, the amount of venous contrast is minimized during the middle of the imaging time when k space for the central partitions is acquired. To help avoid the error of injecting too early, we did not begin the injection (for groups 2–4) until after the acquisition had already begun. We also used a small angiocatheter (22 gauge) to add enough resistance to make an excessively rapid infusion difficult.

Although larger doses of gadolinium chelate (per weight) resulted in greater aortic enhancement (Fig 10), we standardized on a 40-mL dose of contrast material for everyone weighing over 60 kg to simplify the timing of the infusion. The initial use of a different volume of contrast material in every patient based on the patient's weight was confusing and wasted the contrast material that was left over in the bottle. Patients weighing less than 60 kg were given 10, 20, or 30 mL of contrast material to attain a dose per weight of 0.2–0.3 mmol/kg.

One might expect steady-state gradient-echo imaging to be preferable to the spoiled gradient-echo imaging employed here because the long T2 of blood increases the steady-state blood signal. But this effect enhances veins more than arteries because the fast pulsatile flow of arterial blood spoils its steady-state component. In theory, this can then have the paradoxical effect of reduced arterial contrast. In practice, there is little difference between the spoiled and unspoiled techniques. A spoiled gradient-echo pulse sequence was chosen in this study to simplify the theory and analysis by eliminating this potential for differential steady-state magnetization between arterial blood, slower venous blood, and background tissue.

This study of the feasibility of dynamic imaging employed commonly available contrast agents in combination with commonly available imaging hardware and software. Use of faster hardware may permit reduction of the TE, thereby further reducing the number of flow-related phase artifacts. The infusions were performed by hand and could be made more consistent with use of a mechanical injector. Use of a variable infusion rate coordinated with a customized pulse sequence might be preferable, with the center of k space collected during the period of maximum infusion rate. The parts of k space that do not change during gadolinium infusion could be imaged prior to the infusion of gadolinium chelate to minimize the total infusion time and thereby allow an increased infusion rate for the same dose. Imaging with a higher-resolution matrix, such as 512 × 512, may better define small vessel anatomy, permitting more accurate definition of the renal arteries and especially of the accessary renal arteries.

In conclusion, gadolinium-enhanced MR aortography without the confounding effects of excessive venous or background tissue enhancement can be achieved by imaging during intravenous infusion of a paramagnetic contrast agent, which accumulates rapidly and redistributes into the extracellular fluid. ■

Acknowledgments: I thank the MR imaging and angiography fellows and staff at Massachusetts General Hospital, including Christos Athanasoulis, MD, Kent Yucel, MD, John Kaufman, MD, David Harrison, MD, Tom Verdi, MD, Jerry Robins, MD, Bufan Yu, MD, Tom Kinney, MD, Peter Smith, MD, Ben Faitelson, MD, Mitchel Rivitz, MD, Beth Gerard, MD, Arthur Waltman, MD, and Stuart Geller, MD, for the acquisition and interpretation of images and for many helpful discussions. I also thank Joan Frisoli, PhD, Bruce Rosen, MD, PhD, Mark Haacke, MD, Alex Aisen, MD, Bill Palmer, MD, Tom Brady, MD, James Thrall, MD, Mark Cohen, MD, Richard Cambria, MD, Glenn LaMuraglia, MD, Hasan Basari, MD, and Leslie Fang, MD, for many helpful discussions. I thank Mark Kruger, Mary Ellen Korvek, RT, and all of the MR imaging and angiography technologists for technical assistance.

References

1. Potchen JE, Haacke EM, Siebert JE, Gottschalk A. Magnetic resonance angiography: concepts and applications. St Louis, Mo: Mosby, 1993.
2. Edelman RR. MR angiography: present and future. AJR 1993; 161:1–11.
3. Schnall MD, Holland GA, Baum RA, Cope C, Schiebler ML, Carpenter JP. MR angiography of the peripheral vasculature. RadioGraphics 1993; 13:920–930.
4. Lin W, Haacke EM, Smith AS, Clampitt ME. Gadolinium-enhanced high-resolution MR angiography with adaptive vessel tracking: preliminary results in the intracranial circulation. JMRI 1992; 2:277–284.
5. Marchal G, Bosmans H, Van Fraeyenhoven L, et al. Intracranial vascular lesions: optimization and clinical evaluation of three-dimensional time-of-flight MR angiography. Radiology 1990; 175:443–448.
6. Marchal G, Michiels J, Bosmans H, Van Hecke P. Contrast-enhanced MRA of the brain. J Comput Assist Tomogr 1992; 16:25–29.

7. Chakeres DW, Schmalbrock P, Brogan M, Yuan C, Cohen L. Normal venous anatomy of the brain: demonstration with gadopentetate dimeglumine in enhanced 3-D MR angiography. AJR 1991; 156:161–172.
8. Creasy JL, Prince RR, Presbrey T, Goins D, Partain CL, Kessler RM. Gadolinium-enhanced MR angiography. Radiology 1990; 175:280–283.
9. Runge VM, Kirsch JE, Lee C. Contrast-enhanced MR angiography. JMRI 1993; 3:233–239.
10. Prince MR, Yucel EK, Kaufman JA, Harrison DC, Geller SC. Dynamic gadolinium-enhanced 3DFT abdominal MR arteriography. JMRI 1993; 3:877–881.
11. Mirowitz SA, Gutierrez E, Lee JKT, Brown JJ, Heiken JP. Normal abdominal enhancement patterns with dynamic gadolinium-enhanced MR imaging. Radiology 1991; 180:637–640.
12. Matsumoto AH, Teitelbaum GP, Carvlin MJ, Barth KH, Savin MA, Strecker EP. Gadolinium-enhanced MR imaging of vascular stents. J Comput Assist Tomogr 1990; 14:357–361.
13. Sivananthan UM, Rees MR, Ridgway J, Ward J, Bann K. Fast MRI with turbo-FLASH sequences in aortoiliac disease. Lancet 1991; 338:1090–1091.
14. Pavone P, Giuliani S, Cardone G, et al. Intraarterial portography with gadopentetate dimeglumine: improved liver-to-lesion contrast in MR imaging. Radiology 1991; 179:693–697.
15. Losef SV, Rajan SS, Patt RH, et al. Gadolinium-enhanced magnitude contrast MR angiography of popliteal and tibial arteries. Radiology 1992; 184:349–355.
16. Hendrick RE, Roff U. Image contrast and noise. In: Stark DD, Bradley WG, eds. Magnetic resonance imaging. Chicago, Ill: Mosby–Year Book, 1991; 135.
17. Niendorf HP, Haustein J, Cornelius I, Alhassan A, Claub W. Safety of gadolinium-DTPA: extended clinical experience. Magn Reson Med 1991; 22:229–232.
18. Masaryk TJ, Modic MT, Ruggieri PM, et al. Three-dimensional (volume) gradient-echo imaging of the carotid bifurcation: preliminary clinical experience. Radiology 1989; 171:801–806.
19. Wesbey GE, Bergan JJ, Moreland SI, et al. Cerebrovascular magnetic resonance angiography: a critical verification. J Vasc Surg 1992; 16:619–628.
20. Lewin JS, Laub G, Hausmann R. Three-dimensional time-of-flight MR angiography: applications in the abdomen and thorax. Radiology 1991; 179:261–264.
21. Anderson CM, Saloner D, Lee RE, et al. Assessment of carotid artery stenosis by MR angiography: comparison with x-ray angiography and color-coded Doppler ultrasound. AJNR 1992; 13:989–1003.
22. Parker DL, Haacke EM. Signal-to-noise, contrast-to-noise and resolution. In: Potchen EJ, Haacke EM, Siebert JE, Gottschalk A, eds. Magnetic resonance angiography. Boston, Mass: Mosby, 1992; 64.
23. Haustein J, Niendorf HP, Krestin G, et al. Renal tolerance of gadolinium-DTPA/dimeglumine in patients with chronic renal failure. Invest Radiol 1993; 27:153–156.
24. Rofsky NM, Weinreb JC, Bosniak MA, Libes RB, Birnbaum BA. Renal lesion characterization with gadolinium-enhanced MR imaging: efficacy and safety in patients with renal insufficiency. Radiology 1993; 180:85–89.
25. Kim D, Edelman RR, Kent KC, Porter DH, Skillman JJ. Abdominal aorta and renal artery stenosis: evaluation with MR angiography. Radiology 1990; 174:727–731.
26. Debatin JF, Spritzer CE, Grist TM, et al. Imaging of the renal arteries: value of MR angiography. AJR 1991; 157:981–990.